Natural history and biomarkers of retinal dystrophy caused by the biallelic TULP1 variant c.148delG

Majander, Anna

2023-03

Majander , A , Sankila , E-M , Falck , A , Vasara , L K , Seitsonen , S , Kulmala , M , Haavisto , A-K , Avela , K & Turunen , J A 2023 , ' Natural history and biomarkers of retinal dystrophy caused by the biallelic TULP1 variant c.148delG ' , Acta Ophthalmologica , vol. 101 , no. 2 , pp. 215-221 . https://doi.org/10.1111/aos.15252

http://hdl.handle.net/10138/355781
https://doi.org/10.1111/aos.15252

Received: 4 June 2022 | Accepted: 3 September 2022

DOI: 10.1111/aos.15252

Acta Ophthalmologica

ORIGINAL ARTICLE

Natural history and biomarkers of retinal dystrophy caused by the biallelic *TULP1* variant c.148delG

Anna Majander[1] | **Eeva-Marja Sankila**[1] | **Aura Falck**[2] | **Laura Kristiina Vasara**[1] | **Sanna Seitsonen**[1] | **Maarit Kulmala**[1] | **Anna-Kaisa Haavisto**[1] | **Kristiina Avela**[3] | **Joni A. Turunen**[1,4]

[1]Department of Ophthalmology, University of Helsinki and Helsinki University Hospital, Helsinki, Finland

[2]Department of Ophthalmology, PEDEGO Research Unit and Medical Research Center, University of Oulu and Oulu University Hospital, Oulu, Finland

[3]Department of Clinical Genetics, University of Helsinki and Helsinki University Hospital, Helsinki, Finland

[4]Eye Genetics Group, Folkhälsan Research Center, Helsinki, Finland

Correspondence
Dr Anna Majander, Department of Ophthalmology, Helsinki University Hospital, and University of Helsinki, P.O. Box 220, 00029 HUS, Helsinki, Finland.
Email: anna.majander@hus.fi

Abstract

Purpose: To report clinical features and potential disease markers of inherited retinal dystrophy (IRD) caused by the biallelic c.148delG variant in the tubby-like protein 1 (*TULP1*) gene.

Methods: A retrospective observational study of 16 IRD patients carrying a homozygous pathogenic *TULP1* c.148delG variant. Clinical data including fundus spectral-domain optical coherence tomography (SD-OCT) were assessed. A meta-analysis of visual acuity of previously reported other pathogenic *TULP1* variants was performed for reference.

Results: The biallelic *TULP1* variant c.148delG was associated with infantile and early childhood onset IRD. Retinal ophthalmoscopy was primarily normal converting to peripheral pigmentary retinopathy and maculopathy characterized by progressive extra-foveal loss of the ellipsoid zone (EZ), the outer plexiform layer (OPL), and the outer nuclear layer (ONL) bands in the SD-OCT images. The horizontal width of the foveal EZ showed significant regression with the best-corrected visual acuity (BCVA) of the eye ($p < 0.0001$, $R^2 = 0.541$, $F = 26.0$), the age of the patient ($p < 0.0001$, $R^2 = 0.433$, $F = 16.8$), and mild correlation with the foveal OPL-ONL thickness ($p = 0.014$, $R^2 = 0.245$, $F = 7.2$). Modelling of the BCVA data suggested a mean annual loss of logMAR 0.027. The level of visual loss was similar to that previously reported in patients carrying other truncating *TULP1* variants.

Conclusions: This study describes the progression of *TULP1* IRD suggesting a potential time window for therapeutic interventions. The width of the foveal EZ and the thickness of the foveal OPL-ONL layers could serve as biomarkers of the disease stage.

KEYWORDS
early-onset inherited retinal dystrophy, Leber congenital amaurosis, nystagmus, tubby-like protein 1, *TULP1*

1 | INTRODUCTION

Biallelic mutations of the *TULP1* (tubby-like protein 1) gene (OMIM 602280) are a rare cause of inherited retinal dystrophy (IRD) (Banerjee et al., 1998; Hagstrom et al., 1998; Kumaran et al., 2017). Altogether 106 pathogenic or likely pathogenic *TULP1* variants have been associated with the clinical phenotype (www.lovd.nl/gene, access date 10th Jul 2022) that includes nystagmus, night blindness, progressive visual deterioration, maculopathy,

and peripheral pigment retinopathy. The reported features indicate variable severity and progression of the disease classified as Leber congenital amaurosis (LCA, OMIM613843) or early-onset retinal dystrophy (EORD, OMIM600132) depending on the age at onset of visual symptoms (Banerjee et al., 1998; Hagstrom et al., 1998; Kumaran et al., 2017). While the *TULP1* variants have been estimated to account for less than 1% of patients with LCA and EORD, in the Finnish population the *TULP1* variant c.148delG;p.(Glu50AsnfsTer59) is one of the major genetic causes of early childhood-onset IRD with an allele frequency of 0.29% (Avela et al., 2019; Kumaran et al., 2017).

The tubby-like protein 1 is expressed in the cone and rod inner segments (Ikeda et al., 1999; Milam et al., 2000). It is required for the development and survival of photoreceptors being involved in the interaction and transport of specific proteins, like rhodopsin, from the inner segment to the outer segment in photoreceptor cells (Hagstrom et al., 2012). Despite the severe loss of photoreceptors, structural and functional studies on the *TULP1*-associated IRD have indicated the preservation of functionally abnormal foveal cones at an early disease stage (Jacobson et al., 2014).

Recent advances in gene therapies for IRD have raised hope for more effective therapeutic options than currently available, mainly supportive, interventions (Daich Varela et al., 2021). The *TULP1* -associated IRD has been studied on a mouse model (Palfi, Yesmambetov, Humphries, et al., 2020). A recently conducted supplementation therapy trial, targeting photoreceptors in *Tulp1−/−* mouse retinas, demonstrated minimal benefit (Palfi, Yesmambetov, Millington-Ward, et al., 2020). Nevertheless, understanding the natural history and phenotypic characteristics of the disease is required as background information for any future treatments. This study reports clinical features of a single biallelic *TULP1* variant, c.148delG, in 16 patients focusing on potential retinal biomarkers for disease progression. As a reference, we reviewed the visual outcomes of patients carrying other biallelic pathogenic *TULP1* variants retrieved from the literature.

2 | METHODS

This study had ethical and institutional approval by the Helsinki University Hospital, Helsinki, and Oulu University Hospital, Oulu, and its design complied with the Declaration of Helsinki. Patients carrying a homozygous *TULP1* (ENST00000229771, NM_003322.3) c.148delG;p.(Glu50AsnfsTer59) (rs779910894) variants were identified from the paediatric ophthalmology and genetic retina services of the Department of Ophthalmology, and from the Department of Clinical genetics, in the Helsinki and Oulu University Hospitals. The *TULP1* c.148delG gene variant was identified in the diagnostic testing utilizing the gene panels for retinal dystrophy or nystagmus, provided by the accredited molecular genetic laboratories.

The clinical data were retrieved by retrospective review of the study sites' medical records. The following demographic and clinical details were recorded: family history, sex, the age at diagnosis, the presenting sign, the best-corrected visual acuity (BCVA), visual field (VF), spectral-domain optical coherence tomography (SD-OCT) of the optic disc and macula, autofluorescence (AF) images of the retina and the optic disc, and visual electrophysiology. The BCVA initially recorded as Snellen fraction units and visual acuities below chart values were converted to the logMAR units. VFs were studied using Goldmann perimetry. Colour fundus imaging was performed by conventional 35-degree fundus imaging (Topcon TRC-50DX, Topcon Corporation, Tokyo, Japan) or ultra-widefield (200-degree) confocal scanning laser imaging (Optos Panoramic Ophthalmoscope - P200MAAF 200Tx, Dunfermline, United Kingdom). AF imaging was performed using a 30-degree Topcon fundus camera, Spectralis™ (Heidelberg Engineering Ltd, Heidelberg, Germany), or Optos imaging. Full-field electroretinography (ERG) and visually evoked potential (VEP) were recorded incorporating the standards of the International Society for Clinical Electrophysiology of Vision (https://iscev.wildapricot.org/standards).

The Spectralis™ platform was used for SD-OCT imaging. Averaged B-scans of the macula were analysed using the Heidelberg Engineering automated segmentation tool and the manual measuring tool for the assessment of the retinal layer thicknesses and the horizontal width of the ellipsoid zone, respectively. The measurements were performed for the retinal B-scan that horizontally traversed the foveal center since volumetric analyses were not available for patients with labile fixation or nystagmus. The combined thickness of the retinal ganglion cell layer (CGL) and the inner plexiform layer (IPL), and that of the OPL and the ONL, were used for analyses as the anatomical border between the GCL-IPL layers was not clear in all eyes and that of the OPL-ONL depends on the angle between the OCT laser beam and the retinal layers.

A comprehensive literature search on *TULP1*-associated IRD was conducted using the search terms "Tubby-like protein 1", "*TULP1*", "Leber congenital amaurosis", "LCA", "early-onset retinal dystrophy", "EORD" on PubMed (https://www.ncbi.nlm.nih.gov/pubmed/, accessed on 1 June 2022). Only patients with BCVA data, age reported at the time of BCVA assessment and molecular genetic diagnosis were included in the meta-analysis.

The statistical analyses were performed using the SPSS version 25 (Statistical Package of Social Sciences). The SPSS curve estimation module, which compares 11 regression models based on their relative goodness of fit, was used to explore significant correlations among age, BCVA, and the OCT data. The regression model with the lowest significant ($p < 0.05$) P value and the highest F value for the regression, and with the normal distribution of residuals ($p > 0.05$) in the Shapiro-Wilks normality test, was considered as the best fit. Curve estimation and regression analysis were run for the longitudinal BCVA data of both eyes of all patients with the *TULP1* c.148delG gene variant (76 values). For the evaluation of potential markers for the disease stage, the coefficient of variation (CV) was first assessed for the macular

SD-OCT parameters, the patient age and the BCVA at the time of imaging. Potential statistical dependence between the SD-OCT parameters with the highest 25 percentile variation was assessed by the curve estimation and regression analysis. The BCVA of the right eye of the patients retrieved from the literature search and stratified based on the *TULP1* variant type was compared to the first recorded BCVA of the right eye of the *TULP1* c.148delG study group patients using the Independent Samples Kruskal-Wallis test with pair-wise comparisons and adjusted significance by the Bonferroni correction for multiple tests.

3 | RESULTS

Of the recorded 16 patients with *TULP1*-associated IRD, 11 were females and five males. Ophthalmological examinations were performed at the ages between 1 month to 64 years and with the median age of 33 years (range 7–64 years) at the time of the last visit, Table S1. Two patients (P12 and P13) were siblings, and two patients (P9 and P16) were born to distantly consanguineous parents. Nine patients were 12 months of age or younger (range 1–12 months) at the time of their first signs of visual impairment and diagnostic examinations. Their presenting sign was nystagmus and/or head nodding. Another six patients underwent diagnostic examinations due to nyctalopia, subnormal vision for age, or nystagmus somewhat later, at the age of 36–42 months, or "in early childhood" as retrospectively described in their medical records. Patient P16 had her diagnosis of retinitis pigmentosa at the age of 7 years after being symptomatic for a few years. Altogether 11 patients were reported to have nyctalopia at some stage of their disease.

The BCVA of up to 0.2 logMAR was recorded with inter-individual variation and progressive deterioration to the level of light perception as illustrated in Figure 1. Modelling of BCVA deterioration over the follow-up data points of both eyes of all patients resulted the best ($p < 0.0001$) fit for linear regression ($R^2 = 0.506$, $F = 75.8$) with annual BCVA loss of logMAR 0.027. Fitting with the model estimate of the initial mean BCVA of logMAR 0.5, all patients were able to fix and follow as infants.

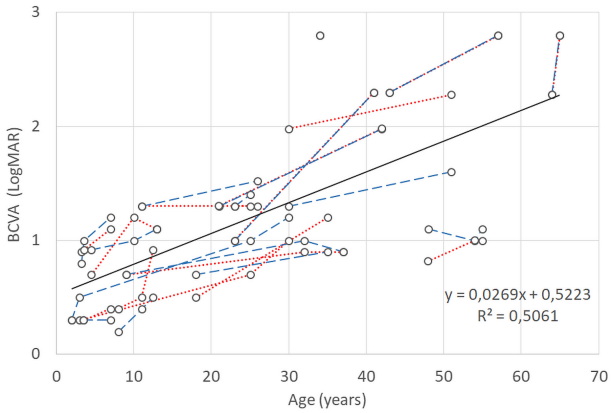

FIGURE 1 The best corrected visual acuity (BCVA) of 16 patients with the biallelic *TULP1* c.148delG variant. The dotted red and the dashes blue lines indicate longitudinal data for the right and left eye of each patient, respectively. The black solid line indicates a linear fit for all BCVA data points.

Ten patients had VF data that showed mild concentric narrowing at the age of 7–10 years, paracentral ring scotoma with or without peripheral visual field remnants at the age of 20–30 years, and progressive concentric narrowing of the visual field to a central five degrees remnant at the age of 48 years. Five youngest patients (P1-7) had full-field ERG data, all showing severely impaired rod and cone responses, or extinguished ERG. Despite impaired ERG responses, patients P1, P6 and P7 studied at the ages 8 to 14 months had some detectable VEP responses.

Patients P1, P3, P4, P7, P8, and P10 had hypermetropic refraction of median + 5.8 diopters (range +3.5 to +6.5 diopters) in childhood, whereas patients P2, P6, P11 and P14 developed moderate to high myopia (range −4.0 to −9.0 diopters). Patients P4 and 14 had strabismus in childhood. Posterior subcapsular cataract was recorded in eight patients at the median age of 35 years (range 18–53 years). Patients P11 and P16 underwent cataract surgery at the age of 30 and 57 years, respectively. Patient P9 was the only one with extraocular disorders, i.e., hypothyreosis, mental problems, sleeping apnea, and obesity.

3.1 | Retinal features

The initial ophthalmoscopy findings were normal in nine patients examined at the age of 12 months or younger. Progressive bull's eye type maculopathy and peripheral pigmentary changes (coarse pigmentation) were recorded from the age of 3 years on. Coarse peripheral pigmentation progressed to bone spicules and retinal atrophy, Figure S1. Patients P13 and P14 also had macular staphyloma at the age of 51 and 54 years, respectively. Twelve patients had some optic disc abnormality. Three patients (P7, P12, P14) had bilateral optic disc drusen that were documented to develop following peripapillary pseudoedema in patient P7, Figure S1A1–A3. Peripapillary retinal nerve fibre layer (RNFL) hypertrophy was revealed by OCT in patient P4, Figure S1b. Four patients had waxy and two pale optic discs.

Ophthalmoscopically detectable maculopathy was reported in all except two patients (P6 and P11) whose retinopathy was recorded as peripheral pigmentary changes and who had not undergone any macular imaging that would have enabled re-review. Maculopathy was characterized by loss of the EZ OCT band beyond the fovea and ONL beyond the macula with primarily preserved inner retinal and pigment epithelial (PE) layers, Figure 2. In two of the studied patients (P12, P16), the EZ was undetectable, and all outer retinal layers had severely abnormal lamination and reflectance. AF imaging of macula showed foveal hypofluorescence surrounded by a perifoveal hyperfluorescent zone, Figure 2. The edges of the central foveal hypofluorescent zone (the nasal edges marked by the yellow arrowheads in the AF images in Figure 2) co-localized with the edges of the remaining foveal EZ (yellow square brackets in the OCT images in Figure 2). Patients P12 and P16 with complete loss of the EZ had a small hyperfluorescent dot in the foveolar center surrounded by an inner

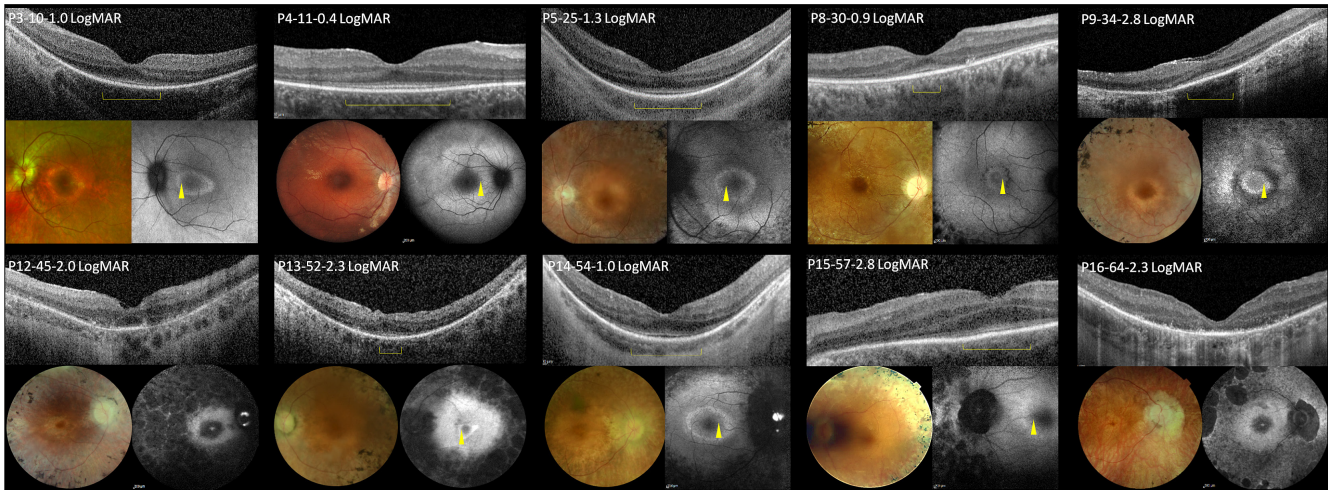

FIGURE 2 Macular spectral-domain optical coherence tomography (SD-OCT), photograph and autofluorencense (AF) images of 10 patients with the biallelic *TULP1* c.148delG variant. The patient number, age in years and the best corrected visual acuity in logMAR at the time of imaging are indicated in each panel of the three images. The horizontal width of the ellipsoid zone is highlighted with the yellow square bracket in the SD-OCT images and the corresponding location of its nasal edge with the yellow arrowheads in the AF images.

hypofluorescent and outer hyperfluorescent zones. In these patients, hypofluorescent areas co-localized with full loss of the outer retinal lamination including the PE in the OCT images. The peripheral retina was characterized by patchy hypofluorescence due to PE atrophy mingled with bone spicules. These peripheral changes were more evident the older the patient. Most eyes also showed peripapillary PE atrophy.

The horizontal width of the residual foveal EZ, the thickness of the retina and selected retinal layers in the foveal center and at 1 mm distance nasal and temporal from the foveal center were assessed by OCT, Table 1. To identify potential markers for disease stage and progression, the degree of variation within the OCT parameters, the BCVA and the patient age at the time of imaging were assessed. Of the OCT parameters, the horizontal width of the EZ, the foveolar OPL-ONL thickness, and the RNFL thickness at 1 mm nasal from the foveal center varied most within the studied 24 eyes of 12 patients with *TULP1* c.148delG variant. The horizontal width of the foveal EZ showed significant common regression with the BCVA of the eye (R^2 =0.541; F = 26.0; p <0.0001) and the age of the patient (R^2 =0.433; F = 16.8; p <0.0001), and weak correlation with the foveolar OPL-ONL thickness (R^2 =0.245; F = 7.2; p = 0.014). Variation of the RNFL thickness in the nasal macula did not show a significant correlation with any of the other OCT parameters, age or BCVA.

3.1.1 | Meta-analysis of vision loss in previously reported patients with TULP1 IRD

Clinical data including BCVA and age at the time of visual acuity assessment were available for 66 previously reported patients with *TULP1* -associated IRD, Table S2. These patients carried 19 different biallelic *TULP1* variants, 10 of which were truncating (43 patients) and 9 missense (23 patients). Four genotypes (six patients) were associated with an infantile-onset disease or LCA and 15 with EORD as the main IRD onset type. The missense variants were associated with less severe visual deterioration than the truncating variants (p = 0.001), Figure 3. The BCVA of the patients with the *TULP1* c.148delG variant did not differ from that of the other truncating *TULP1* variants, and the difference to the missense variants also remained insignificant (p = 0.545 and p = 0.245, respectively). The distribution of ages of patients in these three *TULP1* variant groups did not differ significantly (mean = 19.2 years, SD = 13.2 years, p = 0.827). The historical data on the 19 previously reported *TULP1* variants included only few patients (median = 2, range = 1–16) sharing the same genotype, and it did not provide any longitudinal BCVA or enable age-related regression analysis of individual variants.

4 | DISCUSSION

Two major phenotypes with regards to the age at onset and presenting visual symptoms were associated with the single biallelic *TULP1* variant c.148delG in the 16 patients of this study: LCA with infantile-onset nystagmus and head nodding and EORD with nyctalopia and subnormal vision for age. Both infantile and early childhood disease onset have previously been reported in only three other *TULP1* variants, whereas EORD has been the most frequent disease type (Jacobson et al., 2014; Khan et al., 2015; Lewis et al., 1999; Mataftsi et al., 2007; Wang et al., 2013). However, most of the previous reports include only few patients sharing identical *TULP1* genotypes, which may preclude observation of clinical variation.

The phenotype of patients with the biallelic *TULP1* c.148delG included normal ophthalmoscopy finding in the infantile period converting to progressive maculopathy and peripheral pigmentary retinopathy. Electrophysiology data indicated an early and global loss of photoreceptor function. These features are characteristic of the previously reported *TULP1*-associated disease. Half of our patients also had early-onset cataracts, and one-third marked hypermetropia and hypertrophic optic disc morphology, whereas similar findings have only rarely been reported in association with *TULP1*

TABLE 1 Analysis of variation and regression of the macular spectral-domain optical coherence tomography (SD-OCT) data of 24 eyes of 12 patients with the biallelic *TULP1* c.148delG variant

Analysis of variation

Variable		Mean	SD	Coefficient of variation
SD-OCT layer thickness (μm) at 1 mm distance nasal (N) and temporal (T) from the foveal center	Retina N	305	33	0.11
	Retina T	276	29	0.11
	RNFL N	23	8	**0.35**
	RNFL T	16	4	0.24
	GCL-IPL N	104	19	0.18
	GCL-IPL T	92	16	0.17
	INL N	51	14	0.28
	INL T	48	11	0.23
	OPL-ONL N	63	14	0.22
	OPL-ONL T	61	13	0.21
	Outer retina N	64	15	0.24
	Outer retina T	59	16	0.27
SD-OCT layer thickness (μm) in the foveolar center	Retina	190	43	0.22
	OPL-ONL	81	33	**0.41**
	Outer retina	79	14	0.17
Horizontal width of the EZ in the fovea (μm)		1255	850	**0.68**
BCVA (logMAR)		1.64	0.83	**0.51**
Age at the time of imaging (y)		38	18	**0.48**

Regression analysis (summary of the model with the best fit)

Variable	Age	BCVA	Foveolar OPL-ONL	Foveal EZ width
RNFL N	Cubic R^2 = 0.128 F = 0.9 p = 0.470	S R^2 = 0.079 F = 1.7 p = 0.205	Power R^2 = 0.061 F = 1.3 p = 0.268	Quadratic R^2 = 0.141 F = 1.6 p = 0.236
Foveal EZ width	Logarithmic R^2 = 0.433 **F = 16.8** **p < 0.0001**	Inverse R^2 = 0.541 **F = 26.0** **p < 0.0001**	Power R^2 = 0.245 **F = 7.2** **p = 0.014**	
Foveolar OPL-ONL	Cubic R^2 = 0.172 F = 1.4 p = 0.276	Quadratic R^2 = 0.145 F = 1.8 p = 0.193		

Note: The thickness of the retina selected retinal layers at 1 mm distance nasal (N) and temporal (T) from the foveal center, and in the foveolar center, the horizontal width of the foveal ellipsoid zone (EZ), the best-corrected visual acuity (BCVA) of the imaged eye and the age of the patient at the time of imaging, and the coefficient of variation (CV) for each parameter are presented. Results of the best curve fit for regression of the SD-OCT parameters with the highest variation (CV > 0.32 corresponding to the 75% quartal value shown in bold), the BCVA and the age are presented. Results with statistically significant regression are shown in bold.

Abbreviations: EZ, the ellipsoid zone; GCL-IPL, combined ganglion cell and inner plexiform layers; INL, the inner nuclear layer; ns, not significant; OPL-ONL, combined outer plexiform and outer nuclear layers; RNFL, the retinal nerve fibre layer; SD, standard deviation; y, years.

variants (den Hollander, Lopez, et al., 2007; Hebrard et al., 2011; Jacobson et al., 2014; Khan et al., 2015; Lewis et al., 1999; Mataftsi et al., 2007; McKibbin et al., 2010; Paloma et al., 2000; Verbakel et al., 2019).

Severe loss of the ONL indicating photoreceptor degeneration has previously been documented in the few OCT studies of eyes with *TULP1*-associated IRD and in the *Tulp1*−/− mouse model (Lewis et al., 1999; Palfi, Yesmambetov, Millington-Ward, et al., 2020; Woodard et al., 2021). In accordance with the previous findings, even the youngest patient of the *TULP1* c.148delG study group imaged at the age of 6.5 years showed only a central macular island of normal retinal lamination surrounded by thinned or missing OPL-ONL in the extra-macular zone. However, the extent of the macular changes varied within the study group.

Early maculopathy findings were characterized by variable extra-foveal loss of the EZ and OPL-ONL but preserved inner retinal and PE bands in the SD-OCT images. Parallel assessment of the AF and SD-OCT images suggests the following origin for the bull's eye appearance; the preserved central island of foveal EZ blocks AF of the intact PE that shows increased AF in the perifoveal zone of EZ loss, which is surrounded by fading AF in the outer zone with ONL loss. In the two patients with the most advanced retinopathy and missing detectable EZ, the bull's eye appearance developed mainly due to complete loss of outer retinal lamination and PE. Of the retinal parameters,

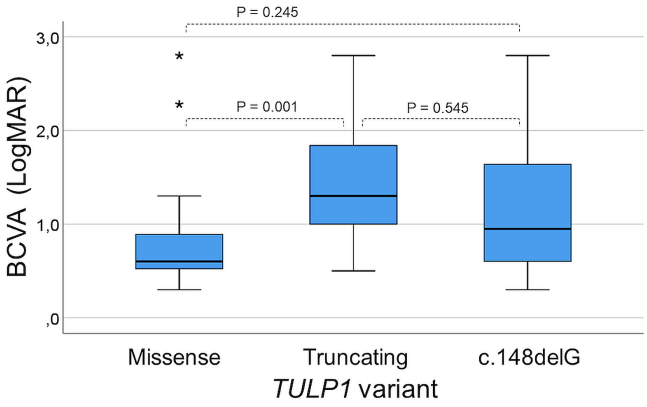

FIGURE 3 The best-corrected visual acuity (BCVA) of the right eye of patients with inherited retinal dystrophy caused by pathogenic *TULP1* variants. Nine different biallelic missense variants were reported in 23 patients and 10 different biallelic truncating variants in 43 patients of the literature search. Sixteen patients with the c.148delG variant were included in the analysis. The study groups were compared using the Independent Samples Kruskal-Wallis test with pairwise comparisons as indicated by the P values for each pair. The two asterisks indicate outliers.

the width of the EZ varied most within the studied eyes and showed significant parallel regression with the BCVA of the eye and the age of the patient, and weak regression with the foveal OPL-ONL thickness suggesting that these findings reflect common structural pathology of varying severity. The width of the foveal EZ and the thickness of the foveal OPL-ONL layers thus serve as structural biomarkers of the preserved foveal photoreceptors and, thereby, of the disease severity and progression.

The EZ reflectance in OCT is thought to be caused by mitochondria in the interface between the inner and outer photoreceptor segments, which is also the site for the expression of the *TULP1* gene and putative function of the tubby-like protein 1 (Ikeda et al., 1999; Milam et al., 2000). The EZ has been used as an indicator of photoreceptor cell integrity and IRD grading e.g. in *GUCY2D* related LCA, whereas the structural and functional findings appeared to be dissociated in the *CEP290* -associated IRD (Bouzia et al., 2020; Valkenburg et al., 2018). In this *TULP1* c.148delG cohort, the foveal EZ width showed a significant correlation with the visual function.

Longitudinal and cross-sectional visual acuity data of the *TULP1* c.148delG cohort showed progressive loss of the BCVA. Modelling of the visual loss suggested linear deterioration with a mean annual loss of logMAR 0.027. The level of visual loss in the *TULP1* c.148delG cohort was similar to that reported in patients carrying other truncating *TULP1* variants, whereas the missense variants appear to show a less devastating effect on visual function. However, there was marked individual variation in the BCVA within the *TULP1* c.148delG cohort as well as in the previously reported case series.

Altogether six patients of the *TULP1* c.148delG cohort had hypertrophic optic disc morphology in the form of optic disc drusen (ODD), pseudoedema, prominent disc margins or prepapillary RNFL thickening. A high level of hypermetropia in three patients may partly explain the observed optic disc morphology, but it hardly explains the conversion of pseudoedema to ODD. There are conflicting reports of an increased prevalence of ODD in IRDs and of the underlying pathogenic mechanisms, but in Usher syndrome, ODD is a frequent finding, and abnormal Usher gene protein is also expressed in retinal ganglion cells providing a potential explanation for the optic disc pathology (Serpen et al., 2020). Although photoreceptors are the site of *TULP1* function, there are evidence of a low-level expression of *TULP1* in human ganglion cells and alterations in ganglion cells of *Tulp1−/−* mice (Milam et al., 2000; Palfi, Yesmambetov, Millington-Ward, et al., 2020). It remains unclear if the observed optic disc changes in this cohort specifically relate to the *TULP1* c.148delG variant or merely reflect some other coincidental genetic background.

This study provides insight into the natural history and phenotypic variation of a single biallelic *TULP1* variant c.148delG, which is both the strength and the weakness of the study. The retinal OCT characteristics are the main study outcome. Applicability of the OCT data to other *TULP1* genotypes may be questioned, but the clinical course of the c.148delG-associated disease shares common features with IRD caused by other *TULP1* variants. This study included all eligible patients carrying the homozygous *TULP1* c.148delG variant from the two university clinics. Due to the rarity of the condition, the number of patients still remained small, which is the main weakness of the study. Therefore, it is possible that a larger study group might have revealed also other biomarkers of disease progression and enabled phenotypic stratification based on the type of disease onset.

Despite the early onset and obvious progressive loss of photoreceptors all patients were able to fix and follow in their infantile period and the central foveal structures were relatively preserved during the first decade of life. This leaves a potential time window for therapeutic interventions. The rarity of the *TULP1* IRD and early disease onset limit the design of prospective natural history studies. However, our data raise an evident need for further characterization of the foveal structure in early childhood. The first gene therapies have recently been applied to IRDs, and research is underway into gene therapy in *TULP1* IRD (Palfi, Yesmambetov, Millington-Ward, et al., 2020). This study adds a detailed phenotypic understanding of the progression of *TULP1* IRD and motivates research and development of therapeutic agents targeted specifically to the foveal rescue.

AUTHOR CONTRIBUTIONS

Research design: AM. Data acquisition and/or research execution: AM, E-MS, AF, LKV, SS, MK, A-KH, KA, JT. Data analysis and/or interpretation: AM, E-MS, AF, JT. Manuscript preparation: AM.

ORCID

Anna Majander https://orcid.org/0000-0001-7145-063X
Anna-Kaisa Haavisto https://orcid.org/0000-0002-6059-9380
Kristiina Avela https://orcid.org/0000-0001-8304-0697
Joni A. Turunen https://orcid.org/0000-0002-9569-9146

REFERENCES

Avela, K., Salonen-Kajander, R., Laitinen, A., Ramsden, S., Barton, S. & Rudanko, S.L. (2019) The aetiology of retinal degeneration in children in Finland – new founder mutations identified. *Acta Ophthalmologica*, 97, 805–814.

Banerjee, P., Kleyn, P.W., Knowles, J.A., Lewis, C.A., Ross, B.M., Parano, E. et al. (1998) TULP1 mutation in two recessive extended Dominican kindreds with autosomal recessive retinitis pigmentosa. *Nature Genetics*, 18, 177–179.

Beryozkin, A., Shevah, E., Kimchi, A., Mizrahi-Meissonnier, L., Khateb, S., Ratnapriya, R. et al. (2015) Whole exome sequencing reveals mutations in known retinal disease genes in 33 out of 68 Israeli families with inherited retinopathies. *Scientific Reports*, 5, 13187.

Bouzia, Z., Georgiou, M., Hull, S., Robson, A.G., Fujinami, K., Rotsos, T. et al. (2020) GUCY2D-Associated Leber congenital amaurosis: A retrospective natural history study in preparation for trials of novel therapies. *American Journal of Ophthalmology*, 210, 59–70.

Daich Varela, M., Cabral de Guimaraes, T.A., Georgiou, M. & Michaelides, M. (2021) Leber congenital amaurosis/early-onset severe retinal dystrophy: Current management and clinical trials. *The British Journal of Ophthalmology*, 105, 1623–1631.

den Hollander, A.I., Lopez, I., Yzer, S., Zonneveld, M.N., Janssen, I.M., Strom, T.M. et al. (2007) Identification of novel mutations in patients with Leber congenital amaurosis and juvenile RP by genome-wide homozygosity mapping with SNP microarrays. *Investigative Ophthalmology & Visual Science*, 48, 5690–5698.

den Hollander, A.I., van Lith-Verhoeven, J.J., Arends, M.L., Strom, T.M., Cremers, F.P. & Hoyng, C.B. (2007) Novel compound heterozygous TULP1 mutations in a family with severe early-onset retinitis pigmentosa. *Archives of Ophthalmology*, 125, 932–935.

Hagstrom, S.A., North, M.A., Nishina, P.L., Berson, E.L. & Dryja, T.P. (1998) Recessive mutations in the gene encoding the tubby-like protein TULP1 in patients with retinitis pigmentosa. *Nature Genetics*, 18, 174–176.

Hagstrom, S.A., Watson, R.F., Pauer, G.J.T. & Grossman, G.H. (2012) Tulp1 is involved in specific photoreceptor protein transport pathways. *Advances in Experimental Medicine and Biology*, 723, 783–789.

Hebrard, M., Manes, G., Bocquet, B., Meunier, I., Coustes-Chazalette, D., Hérald, E. et al. (2011) Combining gene mapping and phenotype assessment for fast mutation finding in non-consanguineous autosomal recessive retinitis pigmentosa families. *European Journal of Human Genetics*, 19, 1256–1263.

Ikeda, S., He, W., Ikeda, A., Naggert, J.K., North, M.A. & Nishina, P.M. (1999) Cell specific expression of tubby gene family members (tub, Tulp1,2, and 3) in the retina. *Investigative Ophthalmology & Visual Science*, 40, 2706–2712.

Jacobson, S.G., Cideciyan, A.V., Huang, W.C., Sumaroka, A., Roman, A.J., Schwartz, S.B. et al. (2014) TULP1 mutations causing early-onset retinal degeneration: Preserved but insensitive macular cones. *Investigative Ophthalmology & Visual Science*, 55, 5354–5364.

Kannabiran, C., Singh, H., Sahini, N., Jalali, S. & Mohan, G. (2012) Mutations in TULP1, NR2E3, and MFRP genes in Indian families with autosomal recessive retinitis pigmentosa. *Molecular Vision*, 18, 1165–1174.

Khan, A.O., Bergmann, C., Eisenberger, T. & Bolz, H.J. (2015) A TULP1 founder mutation, p.Gln301*, underlies a recognisable congenital rod-cone dystrophy phenotype on the Arabian Peninsula. *The British Journal of Ophthalmology*, 99, 488–492.

Kondo, H., Qin, M., Mizota, A., Kondo, M., Hayashi, H., Hayashi, K. et al. (2004) A homozygosity-based search for mutations in patients with autosomal recessive retinitis pigmentosa, using microsatellite markers. *Investigative Ophthalmology & Visual Science*, 45, 4433–4439.

Kumaran, N., Moore, A.T., Weleber, R.G. & Michaelides, M. (2017) Leber congenital amaurosis/early-onset severe retinal dystrophy: clinical features, molecular genetics and therapeutic interventions. *The British Journal of Ophthalmology*, 101, 1147–1154.

Lewis, C.A., Batlle, I.R., Batlle, K.G., Banerjee, P., Cideciyan, A.V., Huang, J. et al. (1999) Tubby-like protein 1 homozygous splice-site mutation causes early-onset severe retinal degeneration. *Investigative Ophthalmology & Visual Science*, 40, 2106–2114.

Mataftsi, A., Schorderet, D.F., Chachoua, L., Boussalah, M., Nouri, M.T., Barthelmes, D. et al. (2007) Novel TULP1 mutation causing Leber congenital amaurosis or early onset retinal degeneration. *Investigative Ophthalmology & Visual Science*, 48, 5160–5167.

McKibbin, M., Ali, M., Mohamed, M.D., Booth, A.P., Bishop, F., Pal, B. et al. (2010) Genotype-phenotype correlation for Leber congenital amaurosis in Northern Pakistan. *Archives of Ophthalmology*, 128, 107–113.

Milam, A.H., Hendrickson, A.E., Xiao, M. et al. (2000) Localization of tubby-like protein 1 in developing and adult human retinas. *Investigative Ophthalmology & Visual Science*, 418, 2352–2356.

Palfi, A., Yesmambetov, A., Humphries, P., Hokamp, K. & Farrar, G.J. (2020) Non-photoreceptor Expression of Tulp1 May Contribute to Extensive Retinal Degeneration in Tulp1−/− Mice. *Frontiers in Neuroscience*, 14, 656. https://doi.org/10.3389/fnins.2020.00656. eCollection.

Palfi, A., Yesmambetov, A., Millington-Ward, S., Shortall, C., Humphries, P., Kenna, P.F. et al. (2020) AAV-Delivered Tulp1 supplementation therapy targeting photoreceptors provides minimal benefit in Tulp1−/− retinas. *Frontiers in Neuroscience*, 14, 891.

Paloma, E., Hjelmqvist, L., Bayés, M., García-Sandoval, B., Ayuso, C., Balcells, S. et al. (2000) Novel mutations in the TULP1 gene causing autosomal recessive retinitis pigmentosa. *Investigative Ophthalmology & Visual Science*, 41, 656–659.

Serpen, J.Y., Prasov, L., Zein, W.M., Cukras, C.A., Cunningham, D., Murphy, E.C. et al. (2020) Clinical features of optic disc drusen in an ophthalmic genetics cohort. *Journal of Ophthalmology*, 2020, 5082706. https://doi.org/10.1155/2020/5082706. eCollection.

Singh, H.P., Jalali, S., Narayanan, R. & Kannabiran, C. (2009) Genetic analysis of Indian families with autosomal recessive retinitis pigmentosa by homozygosity screening. *Investigative Ophthalmology & Visual Science*, 50, 4065–4071.

Ullah, I., Kabir, F., Iqbal, M., Gottsch, C.B., Naeem, M.A., Assir, M.Z. et al. (2016) Pathogenic mutations in TULP1 responsible for retinitis pigmentosa identified in consanguineous familial cases. *Molecular Vision*, 22, 797–826.

Valkenburg, D., van Cauwenbergh, C., Lorenz, B., van Genderen, M.M., Bertelsen, M., Pott, J.W.R. et al. (2018) Clinical characterization of 66 patients with congenital retinal disease due to the deep-intronic c.2991+1655A>G mutation in CEP290. *Investigative Ophthalmology & Visual Science*, 59, 4384–4391.

Verbakel, S.K., Fadaie, Z., Klevering, B.J., van Genderen, M., Feenstra, I., Cremers, F.P.M. et al. (2019) The identification of a RNA splice variant in TULP1 in two siblings with early-onset photoreceptor dystrophy. *Molecular Genetics & Genomic Medicine*, 7, e660. https://doi.org/10.1002/mgg3.660

Wang, X., Wang, H., Sun, V., Tuan, H.F., Keser, V., Wang, K. et al. (2013) Comprehensive molecular diagnosis of 179 Leber congenital amaurosis and juvenile retinitis pigmentosa patients by targeted next generation sequencing. *Journal of Medical Genetics*, 50, 674–688.

Woodard, D.N.R., Xing, C., Ganne, P., Liang, H., Mahindrakar, A., Sankurathri, C. et al. (2021) A novel homozygous missense mutation p.P388S in TULP1 causes protein instability and retinitis pigmentosa. *Molecular Vision*, 27, 179–190.

SUPPORTING INFORMATION

Additional supporting information can be found online in the Supporting Information section at the end of this article.

How to cite this article: Majander, A., Sankila, E-M., Falck, A., Vasara, L.K., Seitsonen, S. & Kulmala, M. et al. (2023) Natural history and biomarkers of retinal dystrophy caused by the biallelic *TULP1* variant c.148delG. *Acta Ophthalmologica*, 101, 215–221. Available from: https://doi.org/10.1111/aos.15252